In these calculations we have had to maintain a temperature above the melting point (e.g., small values of a and b) to prevent the system from crystallizing, so it could be argued that we have failed to model the true thermodynamic state of the amorphous domain. However, it is generally considered that the amorphous material is liquid-like in structure, and if this is the case, the present calculations should be correct. One should also remember, in attempts to apply this work to real systems, that lattice models may not give an accurate representation.

Ironically, these calculations (especially those for $a = b = 0$ and $c > 0$) appear to indicate that entropic forces are acting to favor adjacent and near-adjacent reentry, i.e., by permitting adjacent and near-adjacent reentry the system as a whole can access more configuration space. They seem to support the steric arguments[2] opposing a high degree of random reentry. If the structure of the amorphous domain is indeed liquid-like, then it is impossible for it to contain all the chains available from the two crystal faces. Either there is a high degree of near-adjacent reentry or we do not really understand the structure of the amorphous domain in these polymers.

Recent wide-angle neutron scattering results[19,20] indicate that no more than about four or five adjacent stems within either the (100) or the (010) crystallographic planes belong to the same chain. This is not necessarily inconsistent with the results reported here. From the present calculations we may expect a nonnegligible number of adjacent pairs of stems, but if the probability of finding n adjacent stems behaves something like p^{n-1}, then it will be improbable that any more than a few stems from the same chain be adjacent unless p is very near 1.

Acknowledgment. The author thanks Prof. Marshall Fixman for several helpful discussions and for reviewing the manuscript. This work was supported by the National Institutes of Health, Grant No. GM27945.

References and Notes

(1) *Faraday Discuss. Chem. Soc.* **1979**, *68*, contains the proceedings of a conference in which the major arguments on both sides of the controversy were discussed.
(2) Frank, F. C. *Faraday Discuss. Chem. Soc.* **1979**, *68*, 7.
(3) Guttman, C. M.; DiMarzio, E. A.; Hoffman, J. D. *Polymer* **1981**, *22*, 1466.
(4) Guttman, C. M.; DiMarzio, E. A. *Macromolecules* **1982**, *15*, 525.
(5) Mandelkern, L. *Faraday Discuss. Chem. Soc.* **1979**, *68*, 310.
(6) Sadler, D. M. *Faraday Discuss. Chem. Soc.* **1979**, *68*, 106.
(7) de Gennes, P.-G. "Scaling Concepts in Polymer Physics"; Cornell University Press: Ithaca, NY, 1979.
(8) Flory, P. J.; Yoon, D. Y. *Nature (London)* **1978**, *272*, 226.
(9) Yoon, D. Y.; Flory, P. J. *Faraday Discuss. Chem. Soc.* **1979**, *68*, 288.
(10) Guenet, J. M.; Picot, C.; Benoit, H. *Faraday Discuss. Chem. Soc.* **1979**, *68*, 251.
(11) Stamm, M.; Fischer, E. W.; Dettenmaier, M. *Faraday Discuss. Chem. Soc.* **1979**, *68*, 263.
(12) Sadler, D. M.; Harris, R. *J. Polym. Sci., Polym. Phys. Ed.* **1982**, *20*, 561.
(13) Hoffman, J. D.; Guttman, C. M.; DiMarzio, E. A. *Faraday Discuss. Chem. Soc.* **1979**, *68*, 177. Hoffman, J. D. *Polymer* **1982**, *23*, 656.
(14) Klein, J.; Ball, R. *Faraday Discuss. Chem. Soc.* **1979**, *68*, 198.
(15) DiMarzio, E. A.; Guttman, C. M.; Hoffman, J. D. *Faraday Discuss. Chem. Soc.* **1979**, *68*, 210.
(16) Yoon, D. Y.; Flory, P. J. *Polymer* **1977**, *18*, 509.
(17) Guttman, C. M.; Hoffman, J. D.; DiMarzio, E. A. *Faraday Discuss. Chem. Soc.* **1979**, *68*, 297.
(18) Schelten, J.; Ballard, D. G. H.; Wignall, G. D.; Longman, G.; Schmaltz, W. *Polymer* **1976**, *17*, 751.
(19) Stamm, M. *J. Polym. Sci., Polym. Phys. Ed.* **1982**, *20*, 235.
(20) Wignall, G. D.; Mandelkern, L.; Edwards, D.; Glotin, M. *J. Polym. Sci., Polym. Phys. Ed.* **1982**, *20*, 245.
(21) Mansfield, M. L. *J. Chem. Phys.* **1982**, *77*, 1554.
(22) Balescu, R. "Equilibrium and Nonequilibrium Statistical Mechanics"; Wiley: New York, 1975; pp 273ff.
(23) Dill, K. A. *Faraday Discuss. Chem. Soc.* **1979**, *68*, 106.
(24) Employing only bond flips, as we do in this work, means that states of the system with no parallel bonds are inaccessible. Therefore, these calculations are nonergodic. However, such states probably occupy a negligible fraction of configuration space and the results should not be adversely affected. The author thanks a referee for pointing this out and for giving an example of such an inaccessible state. It is possible that additional questions concerning ergodicity could arise, but none are forseen at this point. See ref 21 for additional details concerning the ergodicity of these calculations.
(25) Cox, D. R.; Miller, H. D. "The Theory of Stochastic Processes"; Wiley: New York, 1965; Chapter 2. The reader is cautioned that this reference contains errors in the random walk treatment (see also ref 3).
(26) Feller, W. "An Introduction to Probability Theory and Its Applications", 3rd ed.; Wiley: New York, 1968; Chapter 14.

Brownian Dynamics Computer Simulations of a One-Dimensional Polymer Model. 1. Simple Potentials

Robert Cook*

Lawrence Livermore National Laboratory, Livermore, California 94550

Lawrence L. Livornese, Jr.†

Department of Chemistry, Lafayette College, Easton, Pennsylvania 18042.
Received November 9, 1982

ABSTRACT: Brownian dynamics computer simulation results are presented on a simple one-dimensional polymer model that contains the essential features of rotational angle flexibility. Comparison is made with analytical treatments of the model.

I. Introduction

In the last few years there have been a significant number of computer simulations of polymeric systems. Many of these simulations use the method of Brownian dynamics, which involves the numerical solution of Langevin equations in order to deal with the diffusive motion of the chain brought about by the solvent. The focus of these studies has been varied. For simple polymethylene-type chains, workers seem to have focused either on the dynamics of conformational transitions[1,2] or upon various relaxation

† Present address: University of Medicine and Dentistry of New Jersey, Newark, NJ.

0024-9297/83/2216-0920$01.50/0

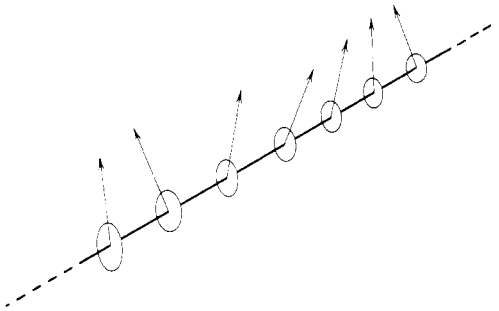

Figure 1. Schematic representation of the one-dimensional polymer model. Each vector can rotate in a plane perpendicular to the common axis; its degree of rotation, ϕ_i, is measured relative to an arbitrary external direction.

properties.[3-5] Some work has also been initiated using Brownian dynamics techniques on polymeric systems of biological interest.[6-8]

In the work presented here we have chosen to explore the relaxation properties of a one-dimensional polymer model, schematically displayed in Figure 1. Our model consists of a series of vectors, each situated in a plane perpendicular to a common axis. The vectors are free to rotate in the plane around the axis, and they interact by way of a nearest-neighbor intervector pair potential. This model, with a simple onefold cosine nearest-neighbor intervector potential, was first studied as a polymer model by Mandell[9] using a high-temperature power series expansion. In this limit (equivalent to a very low barrier to rotation) the model does not display polymer-like susceptibility behavior qualitatively similar to that observed experimentally for various polymer systems. Shore and Zwanzig[10] have studied the same onefold model in the low-temperature (or high barrier) limit by expanding the potential in a power series to quadratic terms and solving the resulting harmonic problem. Numerical calculations of the dynamic susceptibility show qualitative agreement with experimental polymer data, but the high barriers necessary for the quadratic expansion to be a good approximation are not polymer-like. Further, the treatment does not lend itself directly to threefold potentials with polymer-like barriers. Mansfield[11] has recently completed analytical work on the n-fold cosine potential, drawing upon the coupled spring and dashpot model of Clark and Zimm.[12] In the latter approach the coupling of vectors is handled by Hookean springs and the diffusive motion over the barriers by dashpots. Mansfield explores several variations of this theme and obtains results that show some improvement over the work of Shore and Zwanzig, as will be discussed later.

It should be noted that a somewhat different one-dimensional model conceived in the spirit of the one discussed here has been presented by Weiner and Pear[13] in which they essentially project a three-dimensional polymer into one dimension and study the effects of stress on the system. Additionally, simulation studies on a model consisting of a series of vectors independently subject to a threefold rotational potential and coupled by nearest-neighbor quadratic torsional potentials has been studied by Perchak, Yaris, and Skolnick.[14] Analytical work on similar models framed in the methods of soliton physics has also appeared in the literature.[15]

Our motivation for pursuing a one-dimensional model as opposed to a more realistic three-dimensional one is twofold. Our first goal is to provide simulation results on a simple model for comparison with analytical calculations. Second, although there has been a considerable amount of work done with three-dimensional simulations, these models are invariably forced to deal with, or explicitly ignore, such factors as hydrodynamic interaction, excluded volume, and the coupling (or lack thereof) between the various degrees of freedom. This last point has been the subject of considerable discussion[16] and for simple polymer molecules reduces to the question of whether to include terms in the potential to account for bond stretching and bond angle bending vibrations. In doing so, one has to cope with the different time scales for these vibrations and the more interesting conformational motions. Alternatively, one can constrain the more rapid vibrations, thus allowing only torsional bond angle motions. Inclusion of metric tensor terms appears to bring the two methods into agreement for equilibrium calculations but the situation for dynamics is less clear. Though the three-dimensional models are certainly a more faithful representation of the real physical system than a one-dimensional model, they have the disadvantage of making it difficult, if not impossible, to focus on the independent contributions of the various degrees of freedom present, and additionally the computational time for the three-dimensional simulations is often prohibitive. We believe that the one-dimensional model presented here carries with it many of the essential features of polymer rotational angle flexibility and that from it much can be learned, particularly about relaxation properties.

The next section gives a description of the model, the details of the simulation, and the associated calculations. In section III the results of the simulations along with comparisons to the analytical treatments are presented. Section IV offers a brief summary.

II. Model and Computational Methods

We report here the results of Brownian dynamics simulations for both the onefold ($m = 1$) and threefold ($m = 3$) cosine intervector pair potential

$$U = -\frac{EkT}{2}\sum_{i=1}^{N}\cos\,[m(\phi_i - \phi_{i+1})] \tag{1}$$

The barrier to transition from one potential minimum to another is E (for $m = 1$ the wells are in fact the same) and ϕ_i is the direction in an arbitrary external field of vector i. To avoid end effects the N vectors are connected in a ring so that vectors 1 and N are neighbors and the sum in eq 1 is taken appropriately. The threefold potential clearly has similarities to the rotational potential of a simple polymethylene-type polymer and has been used as the rotational potential in three-dimensional simulations, where $\phi_i - \phi_{i+1}$ is taken as the bond rotational angle.[3]

The equation of motion to be solved in a Brownian dynamics simulation is of the form

$$\frac{d^2\phi_i}{dt^2} = -\frac{\partial U}{\partial \phi_i} - \eta\frac{d\phi_i}{dt} + L_i(t) \tag{2}$$

where η is the coefficient of friction associated with the motion of the vector through the solvent and $L_i(t)$ represents the randomly fluctuating force of the solvent on individual vectors. $L_i(t)$ is assumed to be Gaussian with first and second moments given by

$$\langle L_i(t)\rangle = 0 \tag{3}$$

$$\langle L_i(t_1)\cdot L_j(t_2)\rangle = 2kT\delta_{ij}\delta(t_1 - t_2) \tag{4}$$

In the viscous limit where the time steps used, Δt, are much larger than the velocity relaxation times, the acceleration term may be dropped and eq 2 rewritten in a form suitable for computer simulation as

$$\phi_i(t + \Delta t) = \phi_i(t) - \frac{1}{\eta}\frac{\partial U}{\partial \phi_i}\Delta t + \frac{1}{\eta}B_i(\Delta t) \tag{5}$$

where

$$B_i(\Delta t) = \int_0^{\Delta t} L_i(t + s)\, ds \tag{6}$$

$B_i(\Delta t)$ is characterized by a Gaussian probability such that[17]

$$P(B_i(\Delta t)) = (4\pi\eta kT\Delta t)^{-1/2} \exp(-B_i(\Delta t)^2/4\eta kT\Delta t) \tag{7}$$

We will scale the friction coefficient together with the time step by letting

$$\Delta t = (\eta/kT)\Delta\tilde{t} \tag{8}$$

so that eq 5 becomes

$$\phi_i(\tilde{t} + \Delta\tilde{t}) = \phi_i(\tilde{t}) - \frac{1}{kT}\frac{\partial U}{\partial \phi_i}\Delta\tilde{t} + (2\Delta\tilde{t})^{1/2} b_i \tag{9}$$

$B_i(\Delta t)$ is replaced by the scaled b_i, whose values are governed by a Gaussian distribution with variance equal to one.

The simulations were based on eq 9. The gradient of the potential was evaluated at the beginning of each time step and that value used to approximate the potential force throughout the time step. A few test runs were performed in which an effective potential force during the time step was determined iteratively as follows. The potential force calculated at the end of the time step was averaged with the force at the beginning and the step was repeated using the same b_i term. The new final potential was then recycled in the same way until the final position of ϕ_i did not change from trial to trial by more than 1% of the total move. It was found that for time steps $\Delta\tilde{t}$ of 0.01 for the onefold potential and $\Delta\tilde{t}$ of 0.001 for the threefold potentials, nearly all iterations converged in one or two steps, and although there were detectable differences in the trajectories of iterated and noniterated runs, the calculated correlation functions were indistinguishable from one another. Several other test runs were made by halving $\Delta\tilde{t}$ and again the calculated correlation functions were unaffected.

The primary quantity calculated was the correlation function

$$C_n(t) = \langle \cos \phi_i(s) \cdot \cos \phi_{i+n}(s + t) \rangle \tag{10}$$

where n indexes the separation of the two vectors whose correlation is being measured. The autocorrelation would thus be for n equal to zero. This function is of interest since it is the one-dimensional equivalent of the electric moment decay function and is related to the frequency-dependent dielectric response of a polymer through the Fourier transform of its derivative.[18] Specifically

$$\epsilon(\omega) = 1 + 4\pi\chi(\omega) \tag{11}$$

where

$$\chi(\omega) = -\int_0^{\infty} \sum_{n=-l}^{+l} \frac{dC_n(t)}{dt} e^{-i\omega t}\, dt \tag{12}$$

Here, l is a neighbor index sufficiently great such that $C_l(0)$ approaches zero and $C_n(t)$ equals $C_{-n}(t)$. Note that $\epsilon(\omega)$ has both real and imaginary parts

$$\epsilon(\omega) = \epsilon'(\omega) - i\epsilon''(\omega) \tag{13}$$

commonly referred to as the permittivity, $\epsilon'(\omega)$, and loss, $\epsilon''(\omega)$. Graphs of the real vs. imaginary parts of $\chi(\omega)$ (Cole–Cole plots) have characteristic shapes for macromolecules generally described in terms of their deviations from the Debye semicircle that would be obtained if the decay were governed by a single exponential.

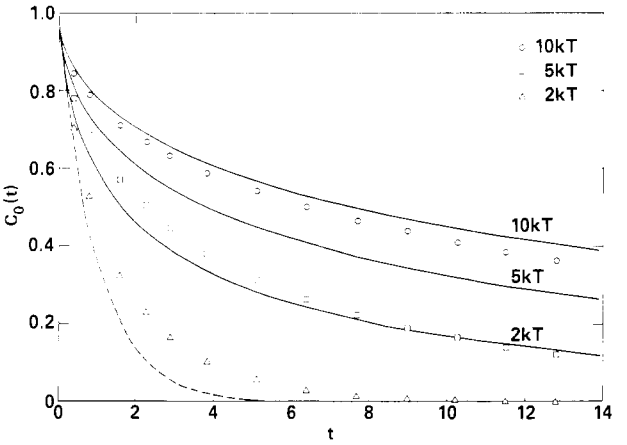

Figure 2. $C_0(t)$ simulation results (open symbols) for the onefold cosine potential (eq 1, $m = 1$). The solid lines are based upon the Shore–Zwanzig calculation (ref 10, eq 34) with the coupling constants shown. The dashed line is $C(t) = \exp(-t)$.

Calculation of the correlation functions from the Brownian dynamics trajectories proceeded as follows. For the simple onefold cosine potential (eq 1, $m = 1$) an initial equilibrium distribution of 100 vectors was generated by Monte Carlo methods and allowed to run for 10 000 steps, and then correlations for $n = 0$–5 were calculated for the next 30 000 steps. This was repeated five times and the obtained correlation functions were averaged. The standard deviation of the correlation data at any time was no more than about 2%. For the threefold cosine potential (eq 1, $m = 3$) 50 trajectories were run, each initialized by Monte Carlo means, in order to sample the configuration space adequately. Taken in sets of 10, the standard deviation was also no more than 2%. The averaged correlations were normalized by dividing by $C_0(0)$. For the onefold case the value of $C_n(0)$, $n = 1, 5$, which is given exactly[10] in terms of Bessel functions by

$$C_n(0) = [I_1(E/2)/I_0(E/2)]^n \tag{14}$$

was found to be within 0.005 of the exact result in all cases. Nearest-neighbor correlations for the threefold case were calculated for a few runs and found to deviate from zero by no more than 0.005.

The susceptibilities were calculated numerically from the autocorrelation data by fitting each successive time interval to the form $C = A \exp(-t/a)$ and calculating the integral in eq 12 analytically for each time interval. The long-time tail was fit by a simple exponential based on the values of A and a for the last time interval. The shapes of the Cole–Cole plots obtained were fairly insensitive to this fit, though the location of the frequency at maximum loss was more so. For the onefold data, calculation of $\chi(\omega)$ was also made by including successive-neighbor correlations.

III. Results[19] and Discussion

The autocorrelation simulation results for the onefold cosine potential with barriers of $2kT$, $5kT$, and $10kT$ are displayed in Figure 2. The results for the Shore–Zwanzig calculation (ref 10, eq 34) are also displayed as is the analytic result for zero barrier height, $C(t) = \exp(-t)$. Agreement is best at the higher barrier heights as one might expect, the $10kT$ Shore–Zwanzig result being only about 10% higher than the simulation results at the longest times calculated. This result indicates that at this barrier height the relaxation of the system is dominated by oscillations in the potential wells rather than by large excursions to the barrier tops. In Figure 3 an example of the neighbor correlation decay is given for the onefold

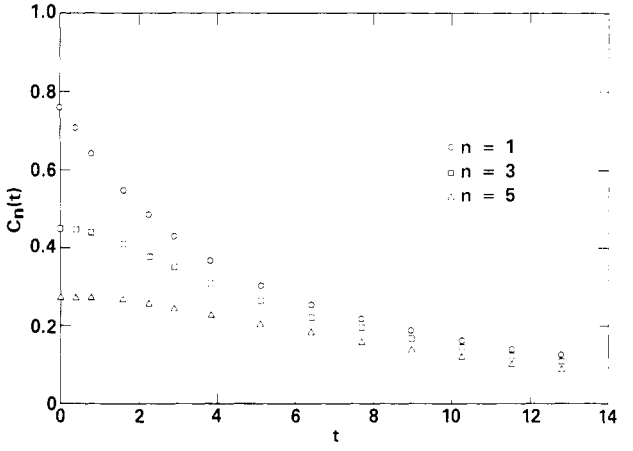

Figure 3. $C_n(t)$ simulation results for n = 1, 3, and 5 for the onefold cosine potential with $5kT$ barriers. Note the initial flatness of the neighbor correlations and the convergence to a single decay at longer times.

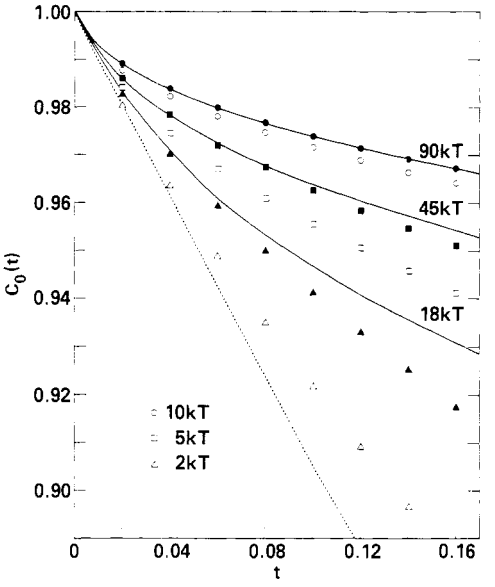

Figure 4. Same as Figure 2 but for the threefold cosine potential (eq 1, m = 3) at short times. The solid symbols are based upon the spring–dashpot calculation of Mansfield.[11]

cosine potential with a $5kT$ barrier. Note the relatively flat neighbor correlation at short times, which contributes very little to the overall susceptibility. The major contribution comes during the later decay when the relaxation curves of all the neighbors converge, the final relaxation being dominated by long-range modes.

The simulation results for the threefold cosine potential with $2kT$, $5kT$, and $10kT$ barriers are displayed (open symbols) in Figures 4 and 5 for short and long times. The appropriate comparison with the Shore–Zwanzig calculation is with coupling constants 9 times as great or $18kT$, $45kT$, and $90kT$, the plots of which are shown. Additionally, the results of Mansfield's calculation with a spring–dashpot model are displayed (closed symbols). Again for $10kT$ barriers, the equivalent Shore–Zwanzig calculation ($90kT$) compares very well with the simulation results, suggesting that very little passage over the barriers is occurring. The spring–dashpot calculations of Mansfield show some improvement at this barrier height at longer times but at short times reproduce the Shore–Zwanzig results. The situation at $5kT$ and $2kT$ is markedly different. The simulation results differ greatly from the Shore–Zwanzig calculation because of the frequent barrier crossing occurring with lower barriers. The Mansfield

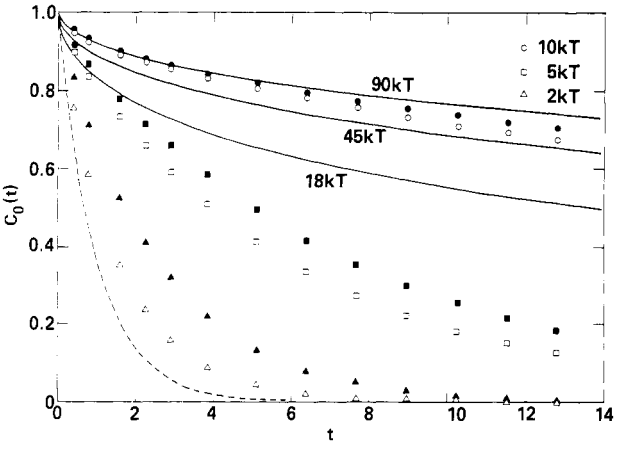

Figure 5. Same as Figure 4 but for long times.

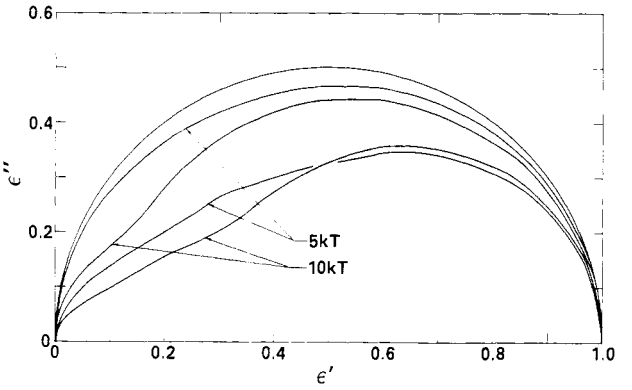

Figure 6. Cole–Cole plots based upon the autocorrelation functions (lower two curves) for the onefold cosine potential at $5kT$ and $10kT$. The Cole–Cole plots with the first five neighbor correlations included (next two curves) are also shown along with a Debye semicircle.

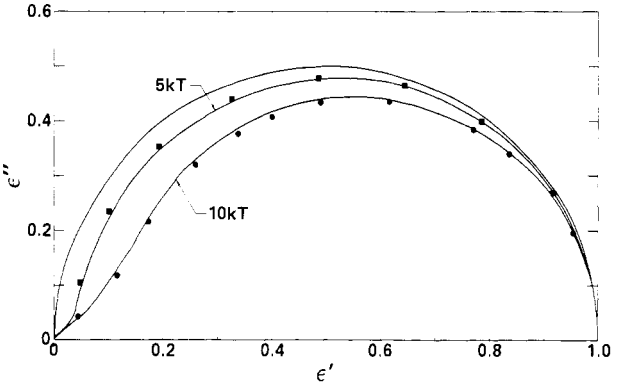

Figure 7. Cole–Cole plots based upon the autocorrelation functions for the threefold cosine potential with $5kT$ and $10kT$ barriers. The solid symbols in this figure represent the spring–dashpot results of Mansfield. A Debye semicircle is also shown.

calculations again follow the Shore–Zwanzig results at very short times but then follow fairly faithfully the simulation results, particularly at the $5kT$ barrier height. Clearly the dashpot aspect of the model is dealing fairly well with the passage over the barriers. The success of the spring–dashpot model at $5kT$ is also encouraging since this barrier height approximates what is typically found in polymer systems.

Cole–Cole plots from the autocorrelation functions for simulations at $5kT$ and $10kT$ are displayed in Figure 6 for the onefold case and in Figure 7 for the threefold case. Figure 6 also shows the Cole–Cole plot obtained by inclusion of the first five neighbor correlations. Cole–Cole

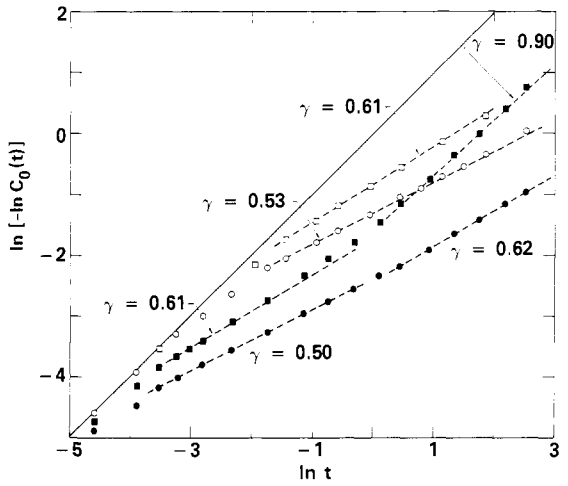

Figure 8. Williams–Watts plots of ln [-ln ($C_0(t)$)] vs. ln t for the $5kT$ (squares) and $10kT$ (circles) barrier heights. The open symbols are for the onefold case and the solid symbols are for the threefold case. The slopes of the data are γ defined in eq 15. A solid line with unit slope that would be obtained from $C(t) = \exp(-t)$ is also shown.

plots based on the spring–dashpot calculation results are also shown in Figure 7. The depression and flattening in relation to the Debye semicircle and the high-frequency "bump", both typical of polymer systems, are clearly evident, particularly for the onefold case. The more accentuated depression in the onefold case is due to the increased time for the correlation function to assume a single-exponential behavior. At very short times all autocorrelations can be characterized by $C(t) = A \exp(-t/a)$ with a equal to 1.0. For the threefold $10kT$ potential, a increases to about 20 in less than 0.8 reduced time units while for the onefold case it takes about 7.5 time units to change the same amount. The more gradually changing exponential decay contributes more to the non-Debye behavior of the Cole–Cole plot, causing a greater depression. Note that inclusion of neighbor correlations for the onefold potential case decreases the asymmetry of the Cole–Cole plot since the neighbor correlations contribute more at higher frequencies due to their initially zero slope. A similar effect was seen by Shore[20] in his treatment of the model.

Attempts to fit the simulation results to the often used Williams–Watts function[21]

$$C(t) = \exp[-(t/a)^{\gamma}] \tag{15}$$

met with only limited success, as can be seen in Figure 8 where ln [-ln ($C(t)$)] is plotted vs. ln t for the $5kT$ and $10kT$ barrier cases. The slope of these lines is thus γ and the intercept at ln t equal to zero is $-\gamma \ln a$. The solid line has unit slope and zero intercept and thus represents the simple Debye exponential decay, $C(t) = \exp(-t)$. As can be seen, the onefold data start by following the simple-exponential form at very short times and then bend out to a fairly linear plot at times greater than about ln t = -2.0. The values of γ are 0.61 and 0.53 for the $5kT$ and $10kT$ onefold data in this region, which is in good agreement with the analytical result of 0.5 from the Shore–Zwanzig calculation. The threefold data appear to have three different behaviors as a function of time. At very short times (not shown) the data behave in accordance with a γ and a of 1.0, reflecting the fact that for very short time the random force term in eq 9 dominates, going as $(\Delta t)^{1/2}$ while the potential term goes as Δt. At slightly longer times a value of γ equal to 0.61 for the $5kT$ and 0.50 for the $10kT$ barrier is seen. This may reflect the steepness of the barrier only, in a manner similar to the Shore–Zwanzig calculation. At longer times, however, a new relaxation mode is available, namely, barrier crossing. This may be governed by a simple exponential form, thus explaining the return of the $5kT$ plot to a γ close to 1.0 at longer times. The rate of barrier crossing in the threefold $10kT$ case is much slower, and correlation functions taken to much longer times may be necessary to see a marked effect as is seen at $5kT$. It should be noted that superimposed on all of this is the size-dependent relaxation mode corresponding to tumbling of all the vectors in concert. This relaxation should go as $\exp(-t/cN)$, c being some time constant (equal to 1 in the Shore–Zwanzig calculation) and N being the number of vectors. To check that this was not a factor in the simulation data presented here, we doubled the system size for a few selected runs; no noticeable effect on the correlation functions was observed.

Another manifestation of this relaxation crossover from one controlling factor to another can be seen by comparing the $5kT$ barrier correlation functions shown in Figures 2 and 4. Note that although the threefold case initially decays more slowly due to the effect of the steeper barrier, at longer times it catches up and ultimately decays more rapidly due to the ability of the vectors in the threefold model to move over the barriers. The success of the spring–dashpot model in treating this multiple-barrier problem may be due to the explicit separation of the torsional motion from the diffusive barrier crossing.

IV. Summary

We have presented correlation function data from computer simulation of a simple one-dimensional polymer model that possesses some of the essential features of rotational angle flexibility. Additionally, Cole–Cole plots calculated from these functions show polymer-like behavior at reasonable barrier heights. The correlation functions from the model with a onefold cosine potential could be fit with some success with the Williams–Watts function; however, for the threefold model distinctly different types of relation processes appear to be occurring at short and long times. Comparison of the simulation results with both the quadratic expansion approach of Shore and Zwanzig and the spring–dashpot calculation of Mansfield has been made, the latter showing significant success in dealing with threefold potentials at moderate polymer-like barrier heights.

Work is now under way to study the effects on the correlation function of modifications of the model. In particular, we are interested in the effect of uneven wells in the threefold case and also the effect of one high barrier in a threefold model, such as exists between the g^+ and g^- states. Incorporation of nonnearest-neighbor effects is also planned.

Acknowledgment. We thank Dr. Marc Mansfield for providing preprints of his work on the spring–dashpot model as well as the results of numerical calculations. Acknowledgment is made to the donors of the Petroleum Research Fund, administered by the American Chemical Society, and also to the Research Corp. for partial support of this work. Part of this work was performed under the auspices of the U.S. Department of Energy by the Lawrence Livermore National Laboratory under Contract W-7405-ENG-48.

References and Notes

(1) Helfand, E.; Wasserman, Z. R.; Weber, T. A. *J. Chem. Phys.* **1979**, *70*, 2016; *Macromolecules* **1980**, *13*, 526.
(2) Pear, M. R.; Weiner, J. H. *J. Chem. Phys.* **1979**, *71*, 212; **1980**, *72*, 3939.

(3) Fixman, M. *J. Chem. Phys.* **1978**, *69*, 1527, 1538.
(4) Weber, T. A. *J. Chem. Phys.* **1978**, *69*, 2347; **1979**, *70*, 4277.
(5) Evans, G. T.; Knauss, D. C. *J. Chem. Phys.* **1980**, *72*, 1504. Evans, G. T. *Ibid.* **1981**, *74*, 4621.
(6) Simon, E. M.; Zimm, B. H. *J. Stat. Phys.* **1969**, *1*, 41.
(7) Levy, R. M.; Karplus, M.; McCammon, J. A. *Chem. Phys. Lett.* **1979**, *65*, 4.
(8) McCammon, J. A.; Northrup, S. H.; Karplus, M.; Levy, R. M. *Biopolymers* **1980**, *19*, 2033. Pear, M. R.; Northrup, S. H.; McCammon, J. A.; Karplus, M.; Levy, R. M. *Ibid.* **1981**, *20*, 629.
(9) Mandell, M. *J. Chem. Phys.* **1972**, *57*, 4858.
(10) Shore, J. E.; Zwanzig, R. *J. Chem. Phys.* **1975**, *63*, 5445.
(11) Mansfield, M. *J. Polym. Sci., Polym. Phys. Ed.*, in press.
(12) Clark, M. B.; Zimm, B. H. In "Dielectric Properties of Polymers"; Karasz, F. E., Ed.; Plenum Press: New York, 1972; pp 45–72. Clark, M. B. *Ibid.*, pp 73–97.
(13) Weiner, J. H.; Pear, M. R. *Macromolecules* **1977**, *10*, 317.
(14) Perchak, D., private communication.
(15) Skinner, J. L.; Wolynes, P. G. *J. Chem. Phys.* **1980**, *73*, 4015, 4022.
(16) Helfand, E. *J. Chem. Phys.* **1979**, *71*, 5000. Chandler, D.; Berne, B. J. *Ibid.* **1979**, *71*, 5386. Pechukas, P. *Ibid.* **1980**, *72*, 6320. Helfand, E.; Wasserman, Z. R.; Weber, T. A.; Skolnick, J.; Runnels, J. H. *Ibid.* **1981**, *75*, 4441. Fixman, M. *Proc. Natl. Acad. Sci. U.S.A.* **1974**, *71*, 3050; see also ref 2.
(17) Chandresekhar, S. *Rev. Mod. Phys.* **1943**, *15*, 1.
(18) Zwanzig, R. *Annu. Rev. Phys. Chem.* **1965**, *16*, 67.
(19) Numerical tabulations of the simulation-generated correlations are available from R.C.
(20) Shore, J. E. Ph.D. Thesis, University of Maryland, 1974.
(21) Williams, G.; Watts, D. C. *Trans. Faraday Soc.* **1970**, *66*, 80. Williams, G.; Watts, D. C.; Dev, S. B.; North, A. M. *Ibid.* **1971**, *67*, 1323.

Characteristic Ratios of Atactic Poly(vinylethylene) and Poly(ethylethylene)

Xu Zhongde,[1a] Nikos Hadjichristidis,[1b] José M. Carella,[1c] and Lewis J. Fetters*[1d]

Department of Modern Chemistry, The University of Science and Technology of China, Hefei, Anhui 230029, People's Republic of China, Department of Industrial Chemistry, The University of Athens, Athens (144), Greece, Department of Chemical Engineering, Northwestern University, Evanston, Illinois 60201, and The Institute of Polymer Science, The University of Akron, Akron, Ohio 44325. *Received September 15, 1982*

ABSTRACT: The characteristic ratios of atactic poly(vinylethylene) and poly(ethylethylene) have been determined by combining intrinsic viscosity and weight-average molecular weight measurements on a series of near-monodisperse samples. The poly(vinylethylenes) were prepared by the anionic polymerization of 1,3-butadiene while the poly(ethylethylene) samples were the product of the hydrogenation of the poly(vinylethylene) materials. The characteristic ratio for poly(ethylethylene) of 5.3, although not in accord with available experimental values, is in excellent agreement with the predictions of Flory, Mark, and Abe.

Introduction

In a series of studies, the rotational isomeric state (RIS) model has been used[2-12] to evaluate the configurational characteristics of polymethylene, poly(methylethylene), and poly(ethylethylene). For the α-olefinic polymers,[4-12] the unperturbed random-coil configurations were treated on the basis of three rotational states for each backbone bond. Each state was weighed according to the interactions between the methylene, methine, and substituent groups that were separated by either three or four C–C bonds. The treatment was applied to chains having various tacticities for the calculation of the characteristic ratios. More recently, Suter and Flory[13] have examined the conformational energy and configurational statistics of poly(methylethylene) by the use of five rotational states for the chain bonds.

Experimental results for the case of polymethylene[2,14-19] have shown the essential correctness and success of the RIS approach. However, disagreement does exist between experiment[20,21] and theory[7] for the case of atactic poly(ethylethylene) [poly(1-butene)]. Some of these experimental results were based[20] on intrinsic viscosity measurements on samples of apparently unknown polydispersity.

Various bulk polymer properties, e.g., elasticity and optical properties, are dependent upon chain configuration. Recently, Graessley and Edwards[22] have related the plateau modulus of a polymer to its characteristic ratio. Hence, knowledge of this parameter is of value for an understanding of properties other than just the dilute solution unperturbed posture of a polymer chain.

It has been reported[23-25] that the anionic polymerization of butadiene can be carried out to yield virtually 100% 1,2 enchainment. The resulting near-monodisperse poly(vinylethylene) can be then converted by hydrogenation to poly(ethylethylene). This approach was used for the samples examined in this study, which reports our findings regarding the characteristic ratios for the atactic forms of poly(vinylethylene) and poly(ethylethylene). To the best of our knowledge, the RIS approach has not yet been used to calculate the characteristic ratio of the former polymer.

Experimental Section

The polymerization, under vacuum, of 1,3-butadiene was carried out with purified, by distillation, *sec*-butyllithium with cyclohexane as the solvent. The polymerization temperatures were between 10 and 20 °C while the duration of the reactions ranged from 24 to 48 h. Termination was carried out by the addition of methanol. The general procedures followed in these polymerizations have been described elsewhere.[26]

Until recently, it was not possible to prepare virtually 100% poly(vinylethylene) via homogeneous anionic polymerization systems involving the alkali metals. However, the use of bis(piperidinyl)ethane as a "promoter" in concert with butyllithium has been reported[23-25] to lead to the near-quantitative conversion of 1,3-butadiene to poly(vinylethylene). Thus bis(piperidinyl)ethane was used to control the microstructure of the polymers examined in this work. The ratio of promoter to active-center concentration was about 5.

The poly(vinylethylene) polymers were converted to poly(ethylethylene) via hydrogenation. The catalyst was palladium on calcium carbonate.[27] After the change brought about by hy-

0024-9297/83/2216-0925$01.50/0